

Article

The Space-Borne SBAS-DInSAR Technique as a Supporting Tool for Sustainable Urban Policies: The Case of Istanbul Megacity, Turkey

Fabiana Calò ^{1,2,*}, Saygin Abdikan ³, Tolga Görüm ⁴, Antonio Pepe ¹, Havvanur Kiliç ^{2,5} and Füsün Balik Şanlı ²

Received: 7 September 2015; Accepted: 1 December 2015; Published: 5 December 2015

Academic Editors: Zhong Lu, Norman Kerle and Prasad S. Thenkabail

¹ Institute for the Electromagnetic Sensing of the Environment (IREA), National Research Council (CNR) of Italy, via Diocleziano 328, Napoli 80124, Italy; pepe.a@irea.cnr.it

² Department of Geomatic Engineering, Civil Engineering Faculty, Yildiz Technical University, Esenler, Istanbul 34220, Turkey; kilic@yildiz.edu.tr (H.K.); fbaliksanli@gmail.com (F.B.S.)

³ Department of Geomatics Engineering, Engineering Faculty, Bulent Ecevit University, Zonguldak 67100, Turkey; sabdikan@beun.edu.tr

⁴ Geography Department, Istanbul University, Laleli, Istanbul 34459, Turkey; tgorum@gmail.com

⁵ Department of Geotechnic Engineering, Civil Engineering Faculty, Yildiz Technical University, Esenler-Istanbul 34220, Turkey

* Correspondence: calo.f@irea.cnr.it; Tel.: +39 081 7620633; Fax: +39 081 5705734.

Abstract: In today's urbanizing world, home of 28 megacities, there is a growing need for tools to assess urban policies and support the design and implementation of effective development strategies. Unsustainable practices of urbanization bring major implications for land and environment, and cause a dramatic increase of urban vulnerability to natural hazards. In Istanbul megacity, disaster risk reduction represents a challenging issue for urban managers. In this paper, we show the relevance of the space-borne Differential SAR Interferometry (DInSAR) technique as a tool for supporting risk management, and thus contributing to achieve the urban sustainability. To this aim, we use a dataset of high resolution SAR images collected by the TerraSAR-X satellite that have been processed through the advanced (multi-temporal) Small Baseline Subset (SBAS)-DInSAR technique, thus producing spatially-dense deformation velocity maps and associated time-series. Results allow to depict an up-to-date picture of surface deformations occurring in Istanbul, and thus to identify urban areas subject to potential risk. The joint analysis of remotely sensed measurements and ancillary data (geological and urban development information) provides an opportunity for city planners and land professionals to discuss on the mutual relationship between urban development policies and natural/man-made hazards.

Keywords: Differential SAR Interferometry (DInSAR); Small Baseline Subset (SBAS); urban deformations; hazard; risk; urbanization; Istanbul; Turkey

1. Introduction

Megacities [1] are the tangible result of the worldwide urbanization process [2] taking place under the global socio-economic, political and ecological changes [3]. Governance of megacities poses a complex challenge [4] to achieve the goal of sustainable development and city's livability [5]. These large growing cities imply increasing population needs, and political institutions and urban planners have to face with an increase in demand for employment, housing, efficient public transportation, adequate water supply and sanitation systems [6,7]. In addition to physical, economic and sociological aspects, urban management needs also to include the environmental

dimension [8]. Indeed, several environmental issues typically result from heavy urbanization processes, e.g., pressure on forests and water resources [9,10], land-use changes and expansion over unstable slopes and areas prone to ground settlements [11,12].

As a result, megacities became extremely vulnerable to natural and human-made hazards [13,14], leading to increase the associated risk and posing a serious threat to the sustainable development of the cities.

Over the last decades, as a consequence of the Turkey's economic growth and the internal migration process from rural Anatolian areas, Istanbul has experienced a high urbanization rate and a rapid population growth. With around 14 million of inhabitants, it is currently the fifteenth megacity in the world [2,15] and, according to the Istanbul Transportation Master Plan, its population is going to exceed 20 million by the year 2023 [16]. This implies a serious challenge for the Municipality; on one hand to provide residents with all necessary systems, from housing to infrastructures and recreational areas, on the other hand, to ensure environmental sustainability. Furthermore, urbanization-related issues are exacerbated by the complexity of the geological, geotechnical and geophysical setting, making Istanbul one of the most risky metropolitan areas [17–21]. For this reason, Istanbul has been selected as a supersite, *i.e.*, a “site of highest priority to the geo-hazards community in which active single or multiple geological hazards caused by single or multiple sources pose a threat to human population and/or critical facilities” [22]. However, most of the studies on Istanbul have been focused on earthquakes [17,18], which are considered the most relevant hazard in terms of economic and life losses; therefore, the major efforts of the scientific community are addressed to assess the associated risk, in order to improve mitigation strategies [23,24]. To our knowledge, only a few studies have been carried out on the analysis of other geological hazards (e.g., subsidence, mass movements) in Istanbul, mainly relied on field surveys and ground-based measurements, therefore inherent to small urban patches [20]. Moreover, the linkage between urbanization and natural hazards in Istanbul has not yet been fully explored although consensus is definitely emerging that urban development and disasters have an interlinked and mutual relationship [25–27]. Indeed, ground deformations induced by human activities in urban areas may represent a serious threat to private and public assets, and analyses of these man-made hazards should be integrated into urban planning and management strategies to achieve the sustainable development of a city.

Location, extent and rate of urban deformations are key information for the hazard/risk assessment and urban damage prevention/mitigation. However, detecting, measuring and monitoring deformations at megacity scale do not represent a feasible task to be accomplished with conventional *in situ* methods. When available, ground-based datasets are seldom complete, consistent and acquired as time-series, and they usually provide point-wise information on areas of very small extent, thus resulting quite limited in terms of temporal and spatial coverage.

With this respect, remote sensed data acquired by satellite Synthetic Aperture Radar (SAR) sensors and processed through Differential SAR Interferometry (DInSAR) techniques [28] may greatly support risk analysis in megacities, fulfilling the requirements of wide area coverage, high spatial resolution and temporal sampling. DInSAR is, in fact, able to retrieve ground displacements by measuring the phase difference (interferogram) between pairs of SAR data collected over the study area at different times and from sufficiently close orbits of the satellite [29,30]. After the first successful applications aimed at mapping the surface deformation induced by single trigger events, such as earthquakes and volcanic unrest [31,32], DInSAR methodology has reached its full maturity while extended to generate time-series of the Line Of Sight (LOS)—projected displacements through the development of “advanced” multi-temporal DInSAR approaches [33–37]. These advanced methods rely on implementing a proper inversion of sequences of differential SAR interferograms, and can be mainly categorized in the two groups of the Persistent Scatterers (PS) [33,36] and Small Baseline (SB) [34,35] algorithms. In particular, the PS techniques analyze point-like targets that are not significantly affected by decorrelation noise [38], and are suitable to monitor deformation affecting point-wise structures. Conversely, the SB methods allow the investigation of displacements over distributed scatterers (DS) on the ground by selecting a set of SAR data pairs with short baselines. To the latter

group belongs the well-known Small Baseline Subset (SBAS) technique, which allows performing two-scale analyses by exploiting both multi-look [34] and single-look [39] SAR interferograms.

Urban deformation monitoring has greatly benefited from the development of these advanced DInSAR approaches. Indeed, being able to remotely investigate the temporal evolution of ground displacements, these techniques have extensively been applied to the analysis of deformation phenomena induced by natural processes and human activities in urbanized areas [40–52]. With the launch of new space-borne SAR sensors (e.g., TerraSAR-X, COSMO-SkyMed, Sentinel-1), the mapping and monitoring capabilities of the advanced DInSAR techniques have been further improved, owing to the higher spatial resolutions (as small as few meters) and/or reduced revisit times (as short as a few days) of the new systems [50,53,54]. These features may provide city planners and managers with up-to-date data characterized by an unprecedented level of detail, particularly suitable for the analysis of surface deformation in highly dynamic urban settings as megacities.

Within this context, the aim of our work is to discuss the impact of urbanization in terms of induced man-made hazards in Istanbul metropolitan area, and to show the relevance of SAR-based remote sensing techniques as tools for supporting risk management and urban development policies. For the purpose, we use a dataset of SAR images acquired by the German satellite mission of TerraSAR-X, which has been processed through the advanced SBAS-DInSAR technique [34,39] to produce spatially-dense deformation velocity maps and associated time-series. The considerably larger density of measure points detected by processing such high resolution SAR data results particularly suitable to analyze settlements of buildings and infrastructures in highly dense built-up areas.

For our analysis, we adopt a two-scale approach, *i.e.*, we firstly investigate the occurrence of deformations at the city-scale and, after identifying areas with potential risk (*hotspots*), we carry out further analyses at local-scale by exploiting available data (*i.e.*, geological and urban development information) for understanding the causes and defining the triggering mechanisms of urban deformations. In particular, we focus on the peninsula of Golden Horn (Figure 1, black square), which represents the socio-cultural center as well as the major transportation hub of Istanbul. The area also includes several sites declared World Heritage Sites by UNESCO, due to their monuments and historical buildings. Therefore, we retain that major efforts should be addressed to the protection of this area and to the assessment and mitigation of the risks that can potentially affect it.

2. Study Area: Istanbul Megacity

2.1. Urbanization and its Impact on Land

Istanbul is currently the financial, commercial and cultural center of Turkey, and one of the most important megacities in the world. The city, which is composed by 39 districts, is divided by the Bosphorus Strait, a narrow canal connecting Marmara Sea with Black Sea. Bosphorus is a natural boundary between Asia and Europe and makes Istanbul a unique city lying on two continents (Figure 1). Moreover, on the European side the city is again separated by the Golden Horn (Haliç), a 7.5 km long estuary that creates a peninsula where the Old Town is located. Figures 1 and 2 show the urban growth experienced by Istanbul since half of the 1940s, when the main body of the city was constituted by the Golden Horn peninsula and few neighborhoods extending along the Bosphorus Strait [55]. This rapid urbanization and population growth [15,56] have had severe impacts on the environment, heavily threatened by the increased pressure of human activities [57–60].

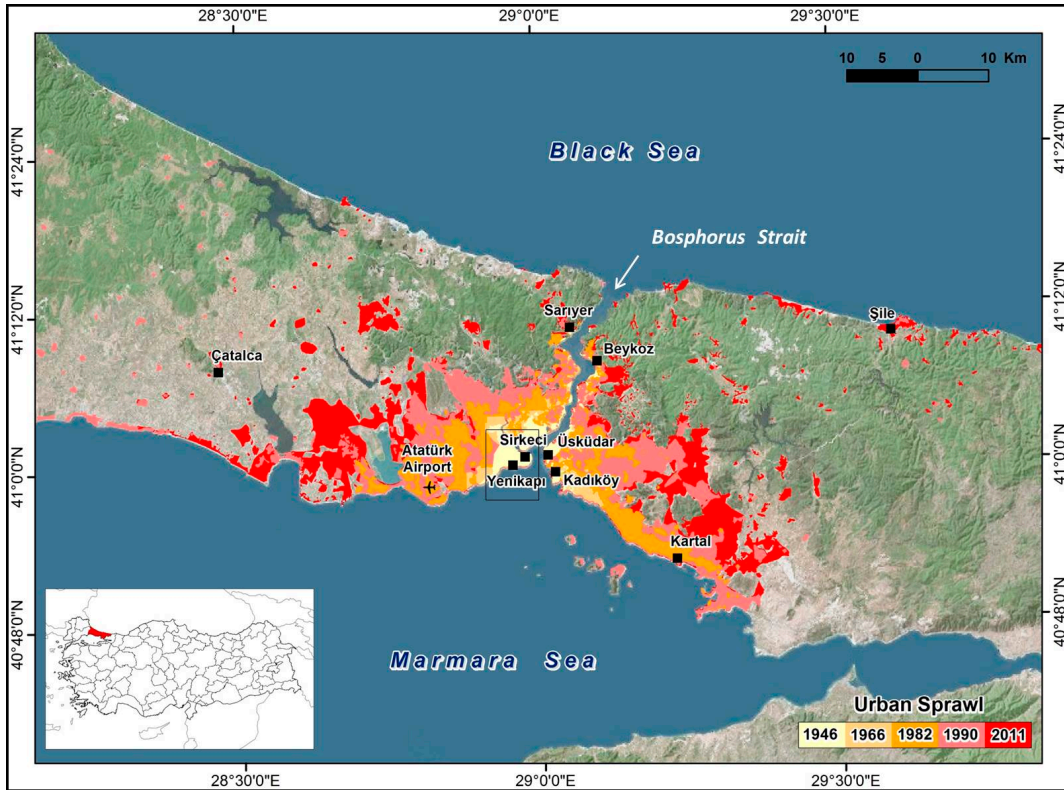


Figure 1. Map showing the temporal and spatial pattern of urbanization for Istanbul megacity, from 1946 to 2011 (adapted from [55]). Black polygon shows location of the Golden Horn peninsula study area.

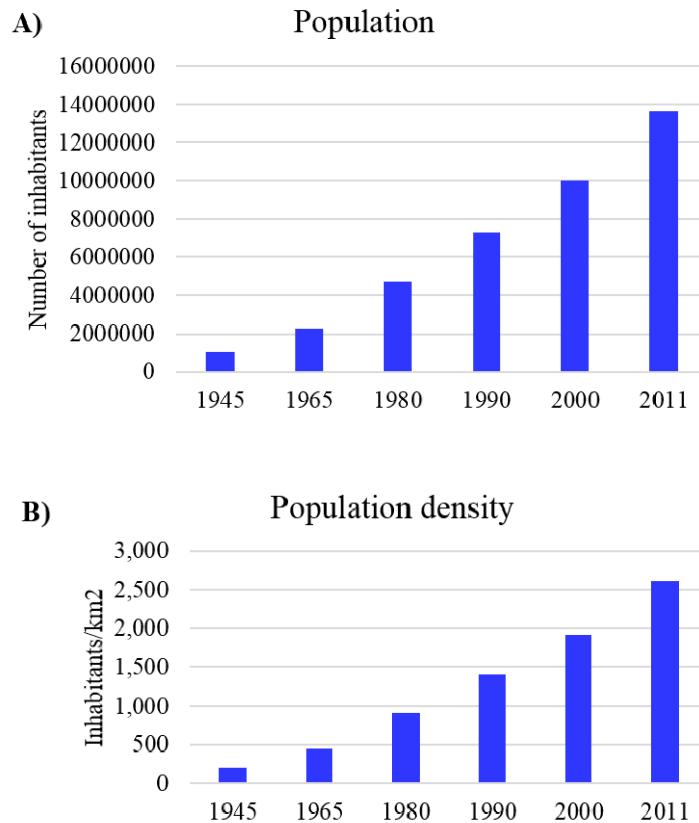


Figure 2. (A) Growth of population and (B) of population density of Istanbul. Data analyzed from 1945 to 2011 [15,56].

Golden Horn is one of the areas of Istanbul that has undergone major changes over time [61–63]. Since the 1950s, because of industrialization the city has been exposed to massive migration from rural Anatolia to the highly industrialized area at Golden Horn. Factories and squatter housing were widespread in the area. In the 1980s, urban renewal projects were implemented to regenerate Golden Horn from an industrial and polluted area into a cultural and recreational waterfront area [62–63]. Sewage systems discharges and industrial facilities were relocated into the city's peripheries, and green parks and recreation areas were developed on both shores (e.g., Miniaturk, a miniature heritage park of Turkey); however, paying little attention to geo-hazards issues. Because of its strategic position, Golden Horn is a major node of transportation in Istanbul, acting as a hub among various sectors of the city. Rapid population growth has led to an increase in demand for public transportation, which has been addressed by enhancing the existing transport systems and developing the new ones. Among the new developed infrastructures, the most challenging is the intercontinental railway project of Marmaray, connecting Asia and Europe through an underwater tunnel [64,65]. This high-budget project has been planned to contribute to reducing traffic congestion and individual use of cars, as well as to mitigate air and noise pollution [66]. Started in 2004, it has become operational since the end of 2013; it is estimated that it will lead the rail use in Istanbul rising from about 3% to 27%, with a total number of approximately 1,5 million passenger journeys per day in 2015 [66]. Marmaray is currently 13.6 km long, including 1.4 km of Bosphorus Crossing Immersed Tunnel, 9.8 km of bored tunnels and 2.4 km of cut-and-cover tunnels [66], and it consists of two surface (Kazlıçeşme and Ayrılık Çeşmesi) and three underground (Yenikapı, Sirkeci and Üsküdar) stations. Among these, Yenikapı station is particularly relevant since it provides interchange between Marmaray, subway and Light Metro, and transfer to sea-buses and tram.

2.2. Geological Setting

The study area is geologically characterized by the presence of Paleozoic, Upper Cretaceous–Lower Eocene, Oligocene, Upper Miocene, Pliocene, Quaternary deposits and Granitic intrusions (Figure 3, [67]). Paleozoic units cover a large area in the geology of the region, including the coastal areas along Marmara Sea and Bosphorus Strait, while in the Istanbul peninsula on the European side, mainly Upper Miocene-aged deposits crop out (Figure 3). Quaternary deposits, mainly observed in the river valleys, are made up of alluviums and man-made fills. Alluvial sediments generally consist of gravel, sand, silt and clay, and range from 5 to 40 m in thickness [68].

Along the Golden Horn inlet, up to Alibey and Kağıthane creeks, alluviums contain normally consolidated clay characterized by high compressibility. Clay formations are interbedded by sand lenses and lenticular masses of gravel formed by previous river flooding [69]. In the area, thickness of these highly heterogeneous alluvial layers ranges from 30 to 35 m.

Quaternary man-made fills are irregularly distributed, and mainly present in the Historical Peninsula where generally overlay the Holocene-aged estuary sediments. These artificial fills are made up mostly of clay, sand, gravel and debris material derived from excavations and demolition of constructions damaged by earthquakes or severe fires devastating the city in the past [70]. Their thickness widely varies in the area, ranging from 7 to 10 m in Yenikapı to approximately 40 m in Sirkeci.



Figure 3. Geological map of Istanbul area (modified after [67]). Red frame shows the footprint of SAR data (TerraSAR-X, descending orbit) used in this study.

3. Data and Method

3.1. The SBAS-DInSAR Technique

The multi-temporal SBAS technique [34] allows detecting Earth surface deformation and analyzing its temporal evolution by generating mean displacement velocity maps and associated time-series. The technique relies on the use of multi-look interferograms generated following a proper selection of interferometric SAR data pairs with short spatial and temporal baselines. The selection is required to mitigate the noise (decorrelation) effects [38] in the generated thus maximizing the number of reliable temporally-coherent pixels (see [71] for the definition of the temporal coherence). However, such a baseline selection may imply that SAR data pairs could be arranged in a few subsets separated each other by large baselines. In the latter case, because there is no suitable interferogram connecting different subsets, they turn out to be independent of each other, thus leading to an underdetermined problem, which is solved by using a Least Squares (LS) minimization based on the Singular Value Decomposition (SVD) method [72]. The SBAS processing chain is also capable to mitigate the impact of possible topographic artifacts that are present in the Digital Elevation Model (DEM) used for the generation of the differential interferograms, which are properly estimated and filtered out. It also improves Phase Unwrapping (PhU) procedure performance by making use of a space-time PhU technique, which takes into account both the and temporal relationships among a stack of multiple interferograms [71,73]. Although originally designed to work at the regional scale using multi-look interferograms, the SBAS approach has subsequently been extended to work with single-look interferograms [39], thus focusing on local deformations affecting single point-wise elements. The analysis at the local scale starts with the modulo- 2π subtraction of previously achieved low-pass phase information, retrieved by analyzing the single-look interferograms, thus providing an estimate of the high-pass (HP) interferometric

phase components. These HP phase components are assumed to be within the $(-\pi, \pi)$ interval, thus avoiding any further unwrapping operation. This two-scale SBAS-DInSAR approach [39] is particularly relevant for urban applications [48,50], allowing us to generate at both scales and deformation velocity maps with different spatial resolutions.

3.2. SAR Data Processing

For the measurement of ground deformations occurring in Istanbul megacity, we applied the SBAS technique to a dataset of 43 TerraSAR-X images collected, between 30 November 2010 and 24 June 2012, along descending orbits. Data were acquired in single HH polarization, Stripmap mode, and were available as SSC (Single-look Slant range Complex) products. Each scene covers an area of approximately 30 km (width) \times 50 km (length), with a 3 m \times 3 m spatial resolution (Figure 3).

Starting from the available SAR images, we generated 129 interferograms with a maximum spatial baseline of 400 m (due to the relatively short time period covered by SAR scenes, no additional constrain has been imposed to the temporal baseline between SAR images). To single out the deformation phase component, we estimated and removed from the interferograms the phase related to the topography of the study area by using a DEM of the area produced from 1/5000 scaled aerial photo-based data with a 5 m \times 5 m spacing and a height accuracy of about 1 m.

Interferograms were phase-unwrapped [71] and properly inverted to perform a time-series analysis [34]. Furthermore, we exploited the capability of the SBAS technique to carry out analyses at two spatial scales, *i.e.*, the regional and local scale [39]. In particular, in the regional scale (*i.e.*, city-scale) analysis, interferograms were averaged by performing a multi-look operation with 10 looks in the range and in the azimuth directions, resulting in a pixel spacing of 30 m (for TerraSAR-X data). Accordingly, a deformation velocity map covering the entire SAR frame with a ground resolution of about 30 m \times 30 m has been produced, providing a synoptic view of the whole investigated area of Istanbul. In contrast, the local scale analysis was carried out using single-look interferograms generated at full spatial resolution (3 m \times 3 m, for TerraSAR-X data), allowing us to reveal deformation patterns that affect single buildings and even portions of buildings (e.g., in case of differential settlements). As a result, deformation maps with a spatial resolution of 3 m \times 3 m covering the higher deformation areas (identified as hotspots in the regional scale analysis) have been produced.

4. Results

The application of the SBAS-DInSAR technique resulted in the production of a spatially-dense deformation velocity map (Figure 4) over the urbanized area of Istanbul. For each SAR measurement point, time-series showing the evolution of displacements in the 2010–2012 observation period have been generated (Figure 5). Displacements are measured along the LOS direction of the satellite. In particular, negative velocity values (red colors) represent movements away from satellite (*i.e.*, land subsidence). The low resolution SBAS-DInSAR map in Figure 4 shows the rate and the spatial pattern of urban deformations, revealing several areas that are affected by subsidence phenomena in Istanbul megacity. Land subsidence is observed in the Kadıköy district (on the Asian side of the city), and in the peripheral neighborhoods of Zeytinburnu and Bakırköy (on the European side), where the International Ataturk Airport is located (Figure 4). These outcomes are in general agreement with a previous study conducted over the area with medium-resolution SAR data acquired by the European Space Agency (ESA) ERS-1/2 and ENVISAT satellites [74]. It is worth pointing out that in these peripheral districts urbanization has resulted in extensive human interventions that have heavily changed the landscape, especially the coastal zones where the seashores have been filled for harbors and recreational parks [75]. Therefore, a further *ad hoc* study should be carried out to assess the risk affecting these neighborhoods where important infrastructures are located.

In this work, we focus on the results achieved over the central districts located along the Golden Horn (Figure 4, black rectangle), and in particular over the Historical Peninsula selected as a relevant case study for being the cultural core of Istanbul, the place that has preserved the identity of the city through the history. High rates of displacements are widely observed in the areas around

the Golden Horn inlet (Figure 5). In particular, two main spatial patterns of land subsidence are detected: (a) along the shores of Golden Horn, a narrow deformation zone extending up to the Alibey and Kağıthane creeks in the North, and (b) in the inland, deformation phenomena characterized by a patchy distribution at the stations of the recent railway transportation system Marmaray, which has become operational since the end of 2013. Analysis of time-series associated to SAR pixels located in these higher deformation areas points out that significant movements, characterized by an average rate exceeding locally 3 cm/year, occur (Figure 5).

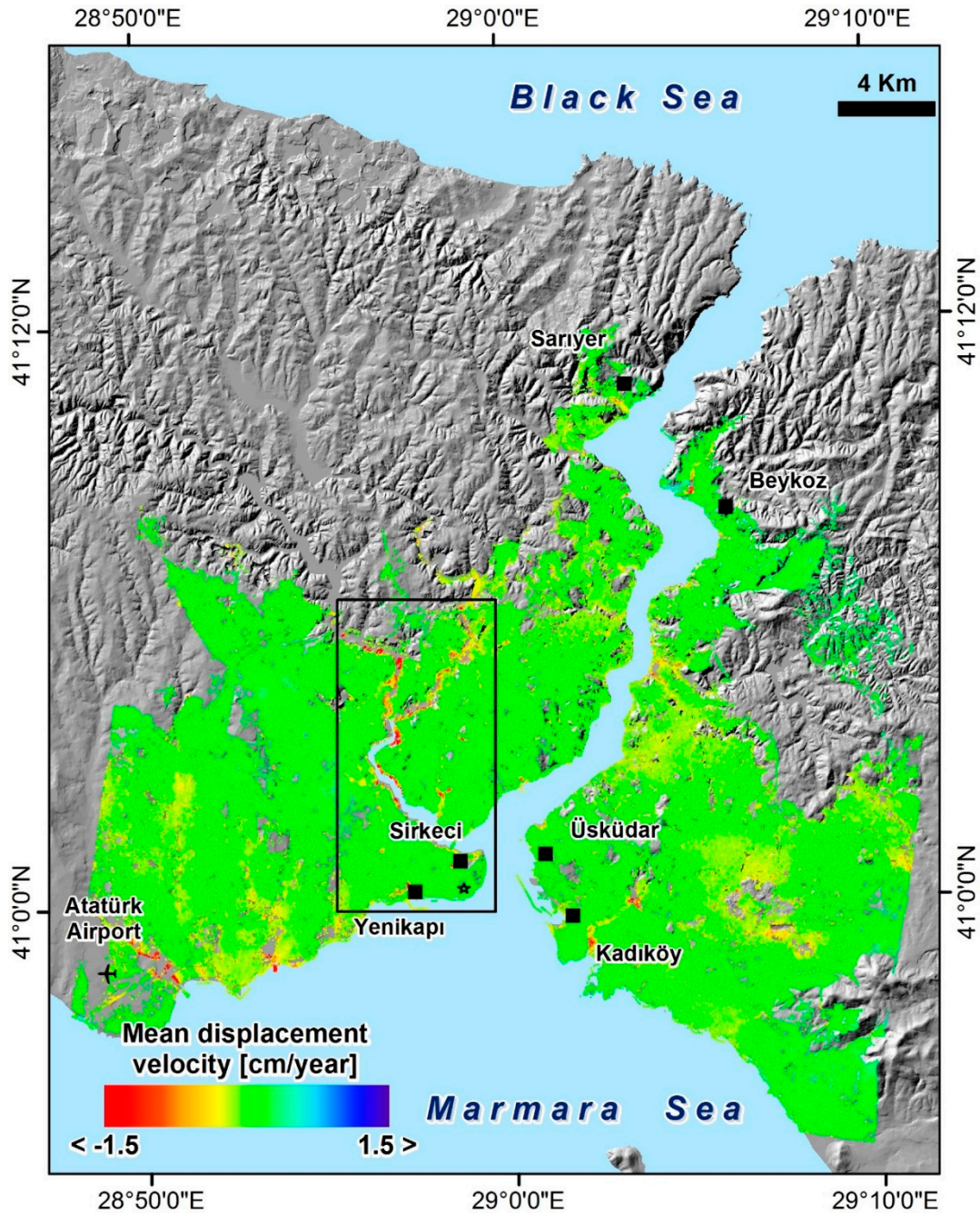


Figure 4. Low resolution deformation velocity map of Istanbul urban area, superimposed on hill shade image derived from DEM. The SBAS-DInSAR map has been obtained by processing TerraSAR-X images acquired in the 2010–2012 time interval. Note that a temporal coherence threshold of 0.8 has been used. Black star shows location of the stable point selected as reference for DInSAR measurements. Black polygon shows location of the study area (see Figure 5).

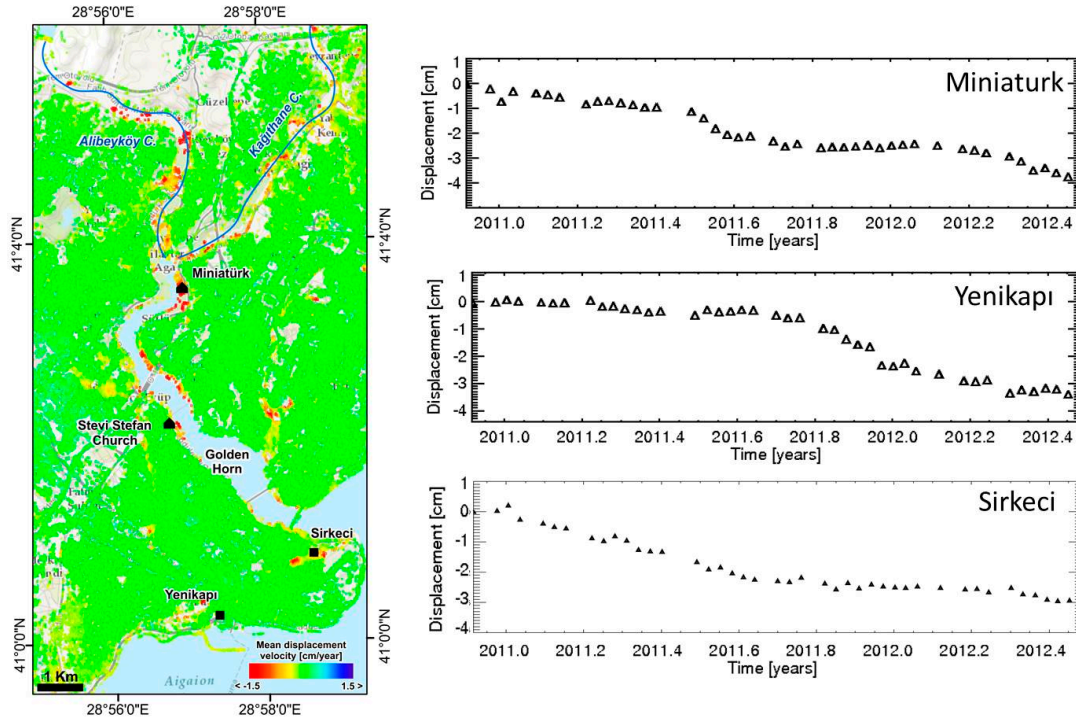


Figure 5. Left: zoomed view of the low-resolution SBAS-DInSAR deformation velocity map, related to the Golden Horn area (for location see Figure 4). Right: time-series of displacements for three unstable SAR measure points located in the artificially filled area of Miniaturk and in the new Marmaray stations of Yenikapı and Sirkeci.

5 Discussion

In this section, we exploit the SAR observations, in conjunction with available geological and urban development information, for the interpretation of the detected deformation phenomena and the correlation with the main driving factors.

Analysis of DInSAR measurements in relation to geological data (Figure 6) reveals that most of land subsidence in Istanbul takes place in the Quaternary layers (alluvial and man-made fills).

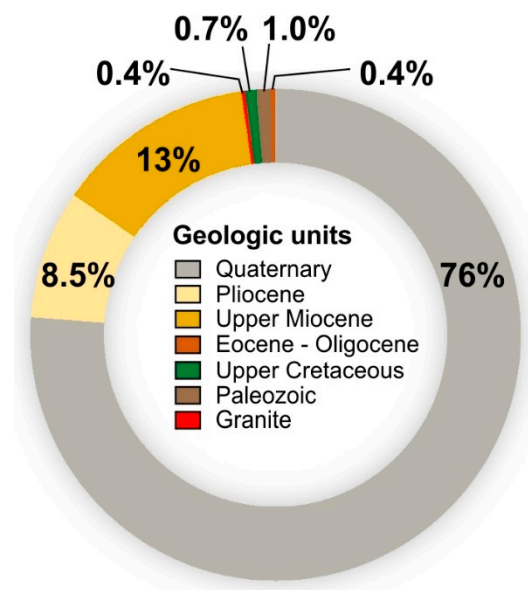


Figure 6. Correlation between urban deformations and geology in Istanbul. Percent values of subsiding SAR pixels for each geologic units are shown.

These lithological complexes, in general highly weathered, are widely present in our study area making it prone to deformation processes (Figures 3 and 5). This is confirmed by the Environmental Impact Assessment Report [76], which points out as the densely built up neighborhoods along the Golden Horn develop on zones at high susceptibility to failures, erosion and subsidence. In such a geological context, urban development, construction of new infrastructures and, more in general, land use changes involving these areas have translated into an increase of vulnerability and risk. Indeed, after projects for the regeneration of urban waterfronts in Istanbul started, the coastline of Golden Horn has undergone heavy changes. Removal of sediments along the shores, in the framework of polluted mud-cleaning works, triggered creep phenomena in the waterfront areas characterized by gentle slopes [77]. Flat areas, about 150 m in width and at an elevation of a few meters a.s.l., were created along the banks, with a high potential risk of flooding. Intense human activity caused subsidence phenomena. Shore zones were filled to create parks and recreational facilities, increasing the risk of subsidence. Among these areas, it is worth mentioning Miniaturk, currently one of the most visited cultural amenities of Istanbul. The park, located on an artificially filled land along the left bank of Golden Horn, covers an area of 60,000 m². Its construction started in 2001 and it was opened to the public in 2003. According to the DInSAR measurements, the park is still suffering cumulated displacements that have approximately reached 4 cm in the observation period of one and a half years (November 2010–June 2012) (Figure 5). This has a relevant economic impact on the Municipality since the park has required a financial investment of approximately \$10 million [63]. Land subsidence has serious consequences along the Golden Horn. In several sites, it has caused severe damage to buildings and infrastructures and, in some cases, it has resulted in the collapse of the ground (Figure 7, [78,79]).

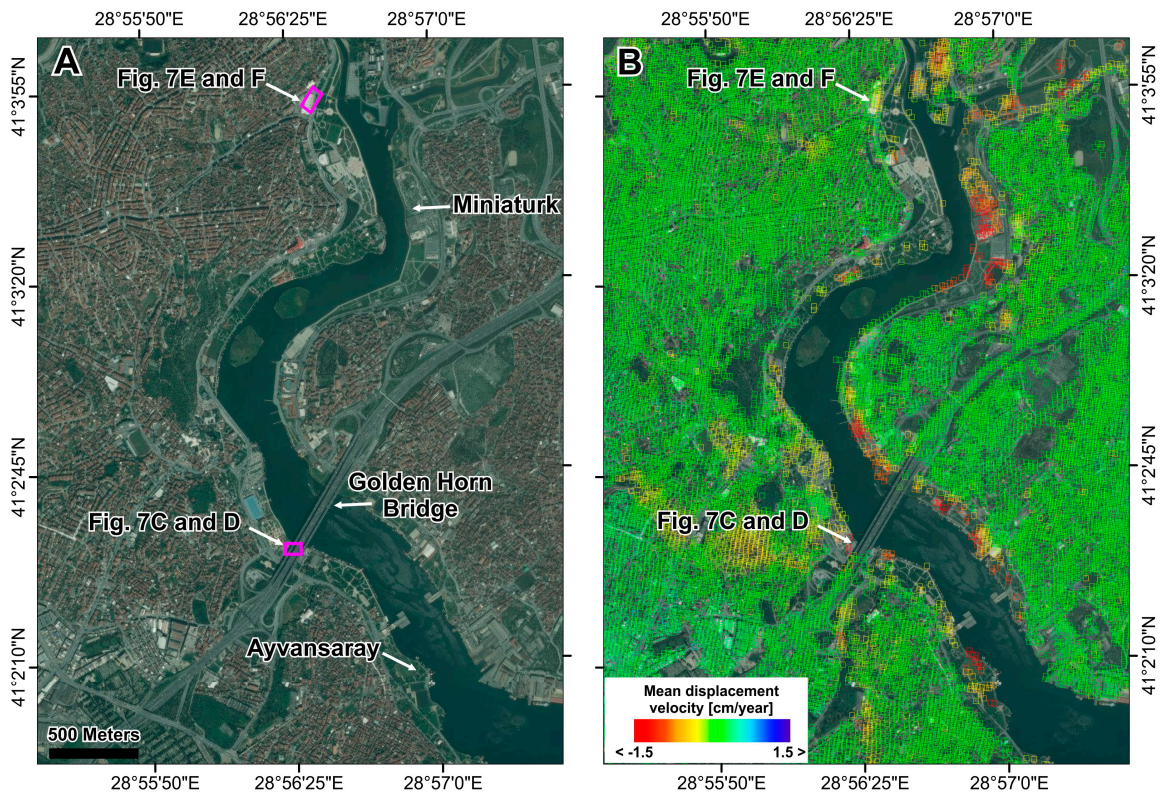


Figure 7. Cont.



Figure 7. (A) Optical satellite image of the Golden Horn and near vicinity. (B) Zoomed view of the low resolution SBAS-DInSAR map, related to the northern neighborhoods along the Golden Horn, including Ayvansaray (UNESCO World Heritage Site). (C,D) Damage observed at the Golden Horn Bridge: displacement affecting a joint of the bridge (C) and the road of south-western part of the bridge (D). (E,F) Ground collapse along the road side at the Silahtaraga Street, Eyup. For location of damaged sites see Figure 7A. Photographs retrieved from Milliyet and Hurriyet Gazetesi [78,79].

Focusing on the Historical Peninsula, comparison of the DInSAR map with a detailed geological map (Figure 8) points out the correlation between the spatial pattern of deformations and the Quaternary deposits. Along the Golden Horn shore, we can observe that deformations occur particularly in areas where the man-made fill layer is characterized by higher thickness and overlays the Haliç formation (see profiles in Figure 8D,F).

This finding is in agreement with studies carried out in the framework of a Golden Horn restoration project started in 1995, which was aimed at defining the geotechnical properties of the Haliç formation. *In situ* investigations and laboratory tests pointed out that the soils were mostly made up of normally consolidated clay characterized by high compressibility, thus susceptible to consolidation processes when loadings are applied [80,81].

Furthermore, the area is characterized by a complex structural setting, due to the presence of several minor faults. In particular, two main fault systems developing along the NW-SE and NE-SW directions dominate the study area (Figure 8). This structural setting contributes to low strength of the soil and, together with poor geo-mechanical properties, acts as predisposing factor on ground instability phenomena that can be triggered by anthropogenic activities.

It can be observed that the Marmaray line partly overlaps with such geological discontinuities at the Sirkeci station, which is affected by significant deformation rates (Figures 5 and 8), suggesting that the role of faulted rocks in the ground instability conditions should be investigated in more details. For this site, we used available *in situ* information to validate the DInSAR observations. Map in Figure 9 shows the full resolution SBAS-DInSAR map relevant to the Sirkeci area and the settlement contour map produced from levelling data [82]. A comparison in terms of displacement rates cannot be performed due to the different periods of analysis (2006–2013 of levelling *vs.* 2010–2012 of DInSAR) and to the non-linear trend of deformations (see time-series of Sirkeci in Figure 5). Furthermore, it is worth noting that the total settlements measured through the levelling

technique include the effect of shaft excavation. However, in terms of spatial distribution and variation of surface deformations (see transition from red to green color in the white continuous-line polygon in Figure 9B), the DInSAR map is in general agreement with the settlement contour map coming out from levelling. In addition, DInSAR measurements allow detecting a further deformation patch along the Marmaray alignment (see white dashed-line polygon in Figure 9B) in an area not covered by ground-based monitoring systems.

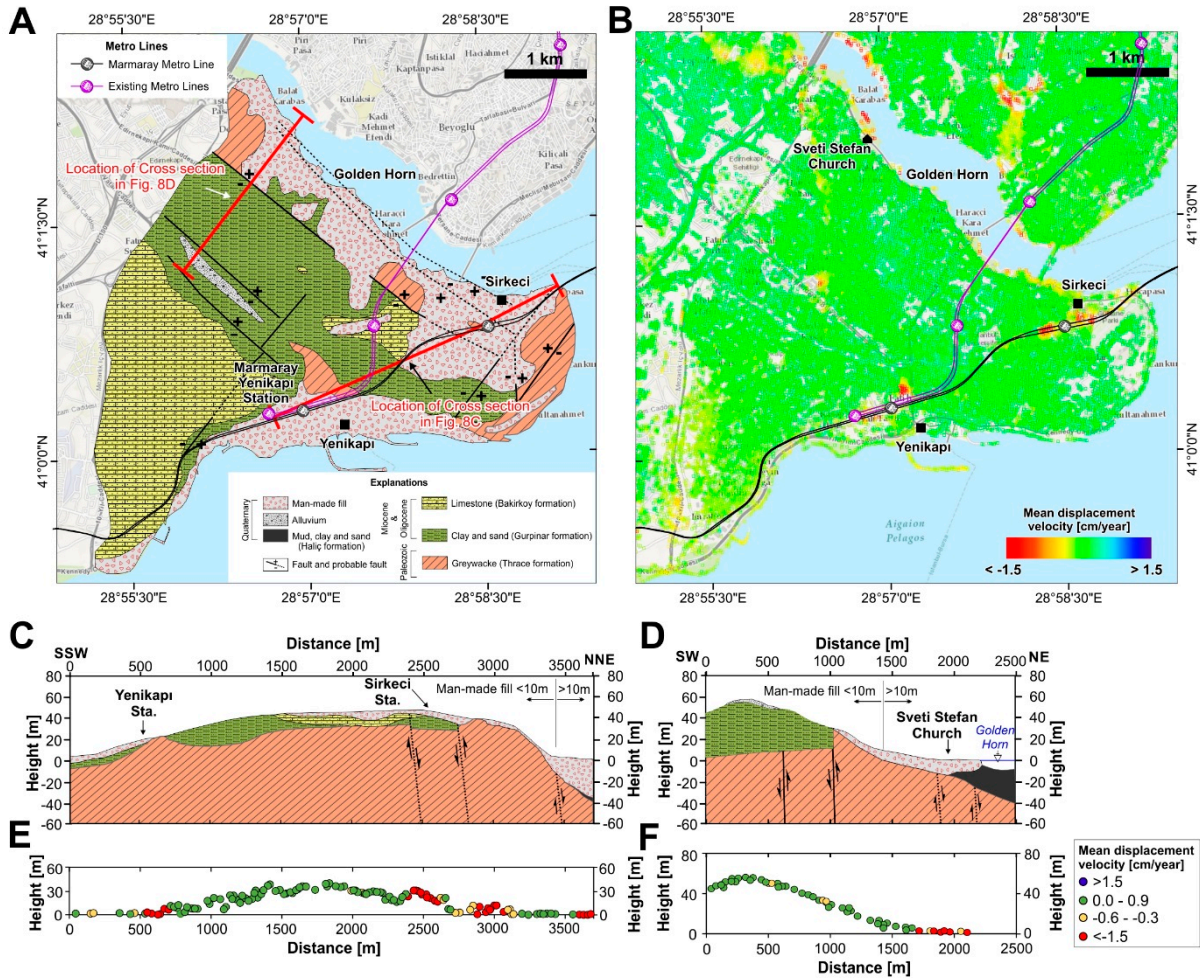


Figure 8. Historical Peninsula of Golden Horn: (A) Detailed geological map (modified after [68]). (B) Low resolution SBAS-DInSAR deformation velocity map. (C,D) Geological cross sections used for the analysis. (E,F) Profiles of DInSAR deformation velocity values along the geological sections in (C) and (D). Note that profiles in (C) and (E) correspond to the Marmaray alignment.

Deformations triggered by underground works are also observed around the excavation area of Yenikapi (Figure 8) and Üsküdar (on the Asian side) stations, with consequent concerns regarding the safety of these high density urban areas, where constructions at surface are very old and usually constituted by series of 5–6 stories buildings, built close to each other, on weak foundations [65]. As a result, they are extremely vulnerable and, therefore, tilting and differential settlements can produce severe structural damage.

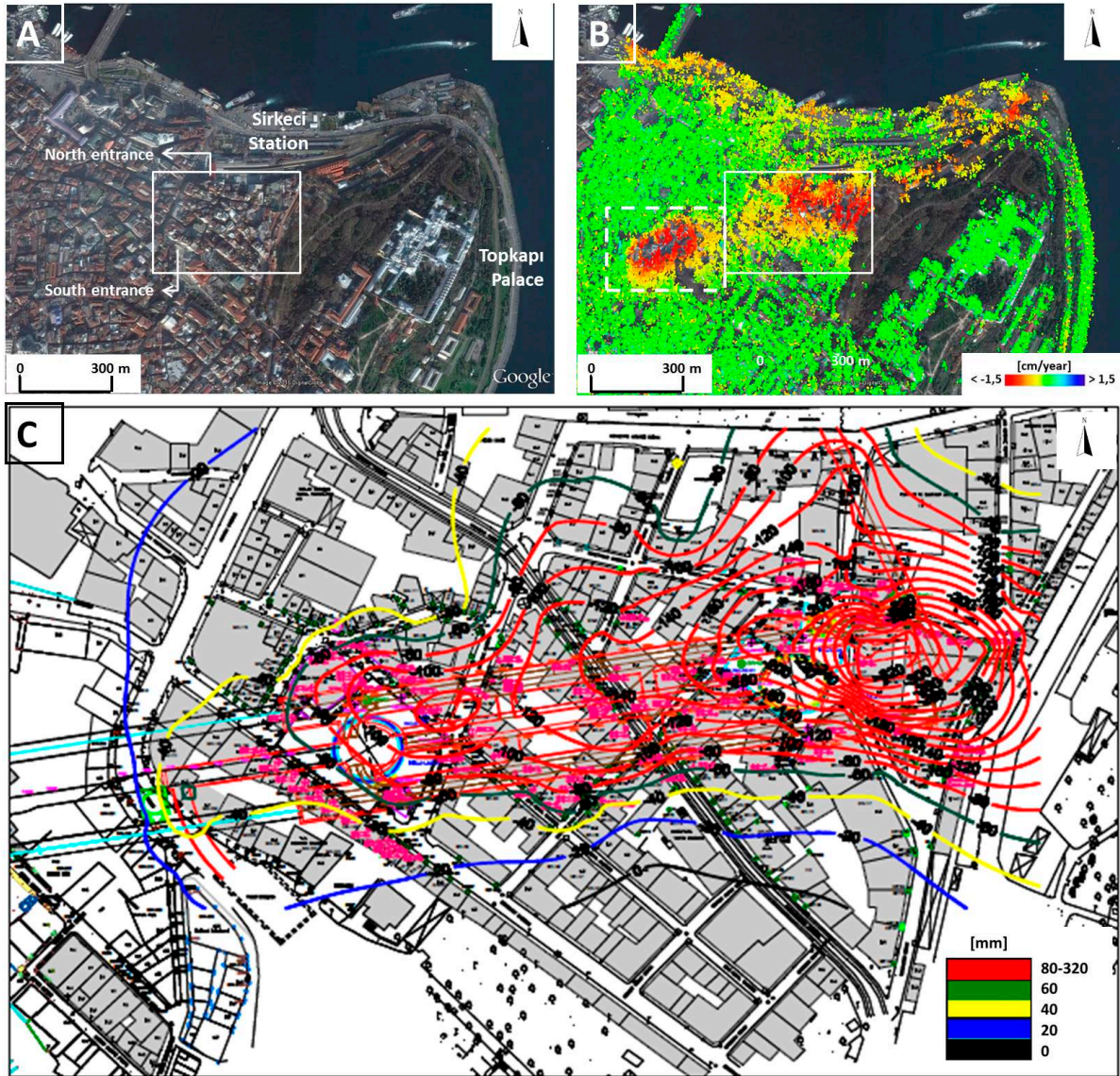


Figure 9. Comparison between SAR and levelling measurements. (A) Optical data related to the Sirkeci area. (B) Corresponding full resolution SBAS-DInSAR deformation velocity map. White continuous-line polygons in (A) and (B) show the area reported in (C). White dashed-line polygon in (B) shows excavation-triggered deformation area detected by DInSAR. (C) Map showing contour lines of cumulated displacements, retrieved from levelling measurements carried out between 10 May 2006 and 2 December 2013. For location of the area see (A,B).

6. Conclusions

Istanbul has been, and still is, affected by intense urbanization and heavy land-use changes, often resulting in increase of geo-hazards and degradation of land. In the worldwide famous Historical Peninsula of Golden Horn, unsustainable development policies have threatened the cultural and historic heritage. Great concerns about the conservation of the area have also been expressed by UNESCO, which has proposed to include it in the List of World Heritage in Danger.

In this work, we complemented the space-borne SBAS-DInSAR technique with geological data and urban development information to investigate the relationship between human activities and ground deformations and to provide a “picture” of potentially risky areas in Istanbul megacity. We particularly focused on the Historical Peninsula, being the most relevant cultural, social and economic space of Istanbul and attracting million visitors from around the world. DInSAR measurements revealed two main patterns of settlements in the area: along the Golden Horn shores,

caused by heavy human-driven changes; along the alignment of the Marmaray railway, related to the recent construction of the new underground stations. Analysis of the SBAS-DInSAR map and associated time-series revealed unknown surface deformations affecting areas not monitored with ground-based instrumentation, pointing out the advantage offered by the high spatial coverage of DInSAR measurements compared to using conventional monitoring techniques that prove to be particularly resource-intensive when the investigation has to cover large urban areas. The results have local and general implications. For Istanbul, selected as a *supersite* owing to the high geophysical risk, the conducted analysis gives new insights on man-made hazards, thus contributing to improve urban risk assessment. The study area is densely built and populated, and also includes most of the historical buildings of Istanbul (e.g., The Blue Mosque and Hagia Sophia), so the availability of continuous and reliable measurements of surface settlements is of crucial importance for the protection of private and public assets as well as of cultural heritage. At global scale, the results provide scientists and city planners with the opportunity to discuss on urbanization issues and increase of urban vulnerability, as well as on the use of space-borne DInSAR techniques for supporting effective urban policies, and contributing to the sustainability of megacities. The increasing availability of SAR data, also free of charge as in the case of the ones provided by the ESA Sentinel-1 mission of the Copernicus programme [83], with the development of reliable and user-friendly processing software, may open the presented approach of analysis to Local Authorities in order to improve urban planning and management. As a final remark, we would like to emphasize that in such a framework the recent implementation of a on-demand web service within the ESA G-POD environment, providing users with automatically retrieved SBAS-DInSAR deformation time-series [84], looks very promising and can be exploited to perform future extended analyses over Istanbul megacity.

Acknowledgments: The work was conducted in the framework of the TUBITAK–2221 Fellowship Program For Visiting Scientists And Scientists On Sabbatical Leave project. TerraSAR-X data were provided by DLR under LAN1708 research project. Taylan Öcalan and Serdar Bayburt provided valuable assistance in data collection. The authors would like to thank four anonymous reviewers for their helpful comments.

Author Contributions: Fabiana Calò carried out SAR data processing and analyses, wrote and revised the manuscript. Saygin Abdikan provided the SAR dataset, contributed to the analysis and manuscript writing. Antonio Pepe supervised the SAR data processing, contributed to the analysis and manuscript writing. Tolga Gorum contributed to the geological, geomorphological analysis and manuscript writing. Havvanur Kilic contributed to the collection and analysis of ancillary data. Fusun Balik Sanli supervised the research development and data collection, contributed to the manuscript writing.

Conflicts of Interest: The authors declare no conflict of interest.

References

1. Kraas, F., Aggarwal, S., Coy M., Mertins G., Eds. *Megacities—Our Global Urban Future*, 1st ed.; Springer: Dordrecht, The Netherlands, 2014; p. 225.
2. United Nations, Department of Economic and Social Affairs, Population Division. World Urbanization Prospects: The 2014 Revision, Highlights (ST/ESA/SER.A/352), 2014. Available online: <http://esa.un.org/unpd/wup/Highlights/WUP2014-Highlights.pdf> (accessed on 3 September 2015).
3. Kraas, F.; Mertins, G. Megacities and global changes. In *Megacities—Our Global Urban Future*, 1st ed.; Kraas, F., Aggarwal, S., Coy, M., Mertins, G., Eds.; Springer: Dordrecht, The Netherlands, 2014; pp. 1–6.
4. Narang Suri, S.; Taube G. Governance in megacities: Experiences, challenges and implications for international cooperation. In *Megacities—Our Global Urban Future*, 1st ed.; Kraas, F., Aggarwal, S., Coy, M., Mertins, G., Eds.; Springer: Dordrecht, The Netherlands, 2014; pp. 195–200.
5. Marsal-Llacuna, M.-L.; Colomer-Llinàs, J.; Meléndez-Fri, J. Lessons in urban monitoring taken from sustainable and livable cities to better address the Smart Cities initiative. *Technol. Forecast. Soc. Chang.* **2015**, *90*, 611–622.
6. Goli, S.; Arokiasamy, P.; Chattopadhyay, A. Living and health conditions of selected cities in India: Setting priorities for the National Urban Health Mission. *Cities* **2011**, *28*, 461–469.

7. Alpkokin, P.; Ergun, M. Istanbul Metrobüs: First intercontinental bus rapid transit. *J. Transp. Geogr.* **2012**, *24*, 58–66.
8. McIntyre, N.E.; Knowles-Yànez, K.; Hope, D. Urban ecology as an interdisciplinary field: Differences in the use of “urban” between the social and natural sciences. *Urban Ecosyst.* **2000**, *4*, 5–24.
9. Atmis, E.; Ozden, S.; Lisec, W. Urbanization pressures on the natural forests in Turkey: An overview. *Urban For. Urban Green.* **2007**, *6*, 83–92.
10. Hossain, F.; Degu, A.M.; Woldemichael, A.T.; Yigzaw W.; Mitra, C.; Shepherd, J.M.; Siddique-E-Akbor, A.H.M. Water resources vulnerability in the context of rapid urbanization of Dhaka City (a South Asian megacity). In *Climate Vulnerability*; Pielke, R.A., Ed.; Academic Press: Oxford, UK, 2013; pp. 393–404.
11. Smyth, C.G.; Royle, S.A. Urban landslide hazards: incidence and causative factors in Niterói, Rio de Janeiro State, Brazil. *Appl. Geogr.* **2000**, *20*, 95–118.
12. Geymen, A.; Baz, I. The potential of remote sensing for monitoring land cover changes and effects on physical geography in the area of Kayisdagi Mountain and its surroundings (Istanbul). *Environ. Monit. Assess.* **2008**, *140*, 33–42.
13. Gencer, E.A. The Interplay between urban development, vulnerability, and risk management. A case study of the Istanbul metropolitan area. *Mediterr. Stud.* **2013**, *7*, doi: 10.1007/978-3-642-29470-9.
14. Kerle, N.; Müller, A. Megacities and natural hazards. In *Encyclopedia of Natural Hazards*; Bobrowsky, P.T., Ed.; Springer: Dordrecht, The Netherlands, 2013; pp. 660–664.
15. Turkish Statistical Institute. Available online: <http://www.turkstat.gov.tr>. (accessed on 3 September 2015).
16. Environmental and Social Impact Assessment for the Eurasia Tunnel Project Istanbul, Turkey; Volume I; Project No. P0106067; Draft report, 2011. Available online: http://www.eib.org/attachments/pipeline/20090678_nts_en.pdf (accessed on 3 September 2015).
17. Parsons, T.; Toda, S.; Stein, R.S.; Barka, A.; Dieterich, J.H. Heightened odds of large earthquakes near Istanbul: An interaction-based probability calculation. *Science* **2000**, *288*, 661–665.
18. Parsons, T. Recalculated probability of $M \geq 7$ earthquakes beneath the sea of Marmara, Turkey. *J. Geophys. Res.* **2004**, *109*, doi:10.1029/2003JB002667.
19. Istanbul, Turkey Disaster Risk Management Profile; 3CD City Profiles Series-Current Working Document: Istanbul, Turkey, 2005; p. 23. Available online: <http://www.urban-response.org/resource/7566> (accessed on 3 September 2015)
20. Duman, T.Y.; Can, T.; Gokceoglu, C.; Nefeslioglu, H.A.; Sonmez, H. Application of logistic regression for landslide susceptibility zoning of Cekmece Area, Istanbul, Turkey. *Environ. Geol.* **2006**, *51*, 241–256.
21. Gencer, E.A. *Natural Disasters, Vulnerability, and Sustainable Development: Examining the Interplay, Global Trends, and Local Practices in Istanbul*; VDM Publishing: Saarbrücken, Germany, 2008; p. 418.
22. Geohazard Supersites—Group on Earth Observations. Available online: supersites.earthobservations.org (accessed on 3 September 2015).
23. Sesetyan, K.; Zulfikar, C.; Demircioglu, M.; Hancilar, U.; Kamer, Y.; Erdik M. Istanbul Earthquake Rapid Response System: Methods and practices. *Soil Dyn. Earthq. Eng.* **2011**, *31*, 170–180.
24. Gunes, O. Turkey’s grand challenge: Disaster-Proof building inventory within 20 years. *Case Stud. Constr. Mater.* **2015**, doi: 10.1016/j.cscm.2014.12.003.
25. World Bank. *Building Safer Cities. The Future of Disaster Risk*; Kreimer, A., Arnold, M., Carlinne, A., Eds.; The World Bank: Washington, DC, USA, 2003; p. 299.
26. Huppert, H.E.; Sparks, S. Extreme natural hazards: Population growth, globalization and environmental change. *Phil. Trans. R. Soc. A.* **2006**, *364*, 1875–1888, doi:10.1098/rsta.2006.1803.
27. Boughedir, S. Case study: Disaster risk management and climate change adaptation in Greater Algiers: Overview on a study assessing urban vulnerabilities to disaster risk and proposing measures for adaptation. *Curr. Opin. Environ. Sustain.* **2015**, *13*, 103–108.
28. Bürgmann, R.; Rosen, P.A.; Fielding, E.J. Synthetic aperture radar interferometry to measure Earth’s surface topography and its deformation. *Ann. Rev. Earth Planet. Sci.* **2000**, *28*, 169–209.
29. Massonnet, D.; Feigl, K.L. Radar Interferometry and its application to changes in the Earth’s surface. *Rev. Geophys.* **1998**, *36*, 441–500.
30. Hensley, S.; Farr, T. Microwave remote sensing and surface characterization. In *Treatise on Geomorphology—Remote Sensing and GIScience in Geomorphology*; Shroder, J., Bishop, M.P., Eds.; Academic Press: San Diego, CA, USA, 2013; Volume 3, pp. 43–79.

31. Massonnet, D.; Rossi, M.; Carmona, C.; Ardagna, F.; Peltzer, G.; Feigl, K.; Rabaute, T. The displacement field of the Landers earthquake mapped by radar interferometry. *Nature* **1993**, *364*, 138–142.
32. Massonnet, D.; Briole, P.; Arnaud, A. Deflation of Mount Etna monitored by spaceborne radar interferometry. *Nature* **1995**, *375*, 567–570.
33. Ferretti, A.; Prati, C.; Rocca, F. Permanent scatterers in SAR interferometry. *IEEE Trans. Geosci. Remote Sens.* **2001**, *39*, 8–20.
34. Berardino, P.; Fornaro, G.; Lanari, R.; Sansosti, E. A new algorithm for surface deformation monitoring based on small baseline differential SAR interferograms. *IEEE Trans. Geosci. Remote Sens.* **2002**, *40*, 2375–2383.
35. Mora, O.; Mallorqui, J.J.; Broquetas, A. Linear and nonlinear terrain deformation maps from a reduced set of interferometric SAR images. *IEEE Trans. Geosci. Remote Sens.* **2003**, *41*, 2243–2253.
36. Werner, C.; Wegmuller, U.; Strozzi, T.; Wiesmann, A. Interferometric point target analysis for deformation mapping. In Proceedings of IEEE International Geoscience and Remote Sensing Symposium, Toulouse, France, 21–25 July 2003; pp. 4362–4364.
37. Hooper, A. A multi-temporal InSAR method incorporating both persistent scatterer and small baseline approaches. *Geophys. Res. Lett.* **2008**, *35*, L16302.
38. Zebker, H.A.; Villasenor, J. Decorrelation in interferometric radar echoes. *IEEE Trans. Geosci. Remote Sens.* **1992**, *30*, 950–959.
39. Lanari, R.; Mora, O.; Manunta, M.; Mallorqui, J.J.; Berardino, P.; Sansosti, E. A small baseline approach for investigating deformation on full resolution differential SAR interferograms. *IEEE Trans. Geosci. Remote Sens.* **2004**, *42*, 1377–1386.
40. Crosetto, M.; Castillo, M.; Arbiol, R. Urban subsidence monitoring using radar interferometry: Algorithms and validation. *Photogramm. Eng. Remote Sens.* **2003**, *69*, 775–783.
41. Lanari, R.; Lundgren, P.; Manzo, M.; Pepe, A. Satellite radar interferometry time series analysis of surface deformation for Los Angeles, California. *Geophys. Res. Lett.* **2004**, *31*, doi: 10.1029/2004GL021294.
42. Cascini, L.; Ferlisi, S.; Fornaro, G.; Lanari, R.; Peduto, D.; Zeni, G. Subsidence monitoring in Sarno urban area via multitemporal DInSAR technique. *Int. J. Remote Sens.* **2006**, *27*, 1709–1716.
43. Lanari, R.; Casu, F.; Manzo, M.; Zeni, G.; Berardino, P.; Manunta, M.; Pepe, A. An overview of the small baseline subset algorithm: A DInSAR technique for surface deformation analysis. *Pure Appl. Geophys.* **2007**, *164*, 637–661.
44. Stramondo, S.; Saroli, M.; Tolomei, C.; Moro, M.; Doumaz, F.; Pesci, A.; Loddo, F.; Baldi, P.; Boschi, E. Surface movements in Bologna (Po Plain—Italy) detected by multitemporal DInSAR. *Remote Sens. Environ.* **2007**, *110*, 304–316.
45. Herrera, G.; Fernandez-Merodo, J.; Tomas, R.; Cooksley, G.; Mulas, J. Advanced interpretation of subsidence in Murcia (SE Spain) using A-DInSAR data-modelling and validation. *Natural Hazard. Earth Syst. Sci.* **2009**, *9*, 647–661.
46. Osmanoglu, B.; Dixon, T.H.; Wdowinski, S.; Cabral-Cano, E.; Jiang, Y. Mexico City subsidence observed with persistent scatterer InSAR. *Int. J. Appl. Earth Obs.* **2011**, *13*, 1–12.
47. Calò, F.; Calcaterra, D.; Iodice, A.; Parise, M.; Ramondini, M. Assessing the activity of a large landslide in southern Italy by ground-monitoring and SAR interferometric techniques. *Int. J. Remote Sens.* **2012**, *33*, 3512–3530.
48. Arangio, S.; Calò, F.; Di Mauro, M.; Bonano, M.; Marsella, M.; Manunta, M. An application of the SBAS-DInSAR technique for the assessment of structural damage in the city of Rome. *Struct. Infrastruct. Eng.: Maint. Manag. Life-Cycle Des. Perform.* **2013**,. doi: 10.1080/15732479.2013.833949.
49. Chaussard, E.; Amelung, F.; Abidin, H.; Hong, S.-H. Sinking cities in Indonesia: ALOS PALSAR detects rapid subsidence due to groundwater and gas extraction. *Remote Sens. Environ.* **2013**, *128*, 150–161.
50. Calò, F.; Ardizzone, F.; Castaldo, R.; Lollino, P.; Tizzani, P.; Guzzetti, F.; Lanari, R.; Angeli, M.C.; Pontoni, F.; Manunta, M. Enhanced landslide investigations through advanced DInSAR techniques: The Ivancich case study, Assisi, Italy. *Remote Sens. Environ.* **2014**, *142*, 69–82.
51. Peduto, D.; Cascini, L.; Arena, L.; Ferlisi, S.; Fornaro, G.; Reale, D. A general framework and related procedures for multiscale analyses of DInSAR data in subsiding urban areas. *ISPRS J. Photogramm. Remote Sens.* **2015**, *105*, 186–210.
52. Zhao, Q.; Pepe, A.; Gao, W.; Lu, Z.; Bonano, M.; He, M.; Tang, X. A DInSAR Investigation of the Ground Settlement Time Evolution of Ocean-Reclaimed Lands in Shanghai. *IEEE Sel. Top. Appl. Earth Obs. Remote Sens.* **2015**, doi:10.1109/JSTARS.2015.2402168.

53. Cascini, L.; Peduto, D.; Reale, D.; Arena, L.; Ferlisi, S.; Fornaro, G. Detection and monitoring of facilities exposed to subsidence phenomena via past and current generation SAR sensors. *J. Geophys. Eng.* **2013**, doi:10.1088/1742-2132/10/6/064001.
54. Sansosti, E.; Berardino, P.; Bonano, M.; Calò, F.; Castaldo, R.; Casu, F.; Manunta, M.; Manzo, M.; Pepe, A.; Pepe, S.; Solaro, G.; Tizzani, P.; Zeni, G.; Lanari, R. How second generation SAR systems are impacting the analysis of ground deformation. *Int. J. Appl. Earth Obs. Geoinf.* **2014**, *28*, 1–11.
55. Doker, F.M. Determining, Monitoring and Modelling the Urban Growth of Istanbul. PhD Thesis, Istanbul University, Istanbul, Turkey, 2012.
56. Murat, S. Kadıköy'ün Nüfus ve Eğitim Yapısı. In Proceedings of Sosyal Siyaset Konferansları, 52. Kitap, İ.Ü. Yayın No. 4669, Istanbul, Turkey, 2007.
57. Kaya, S.; Curran, P.J. Monitoring urban growth on the European side of the Istanbul metropolitan area: A case study. *Int. J. Appl. Earth Obs. Geoinf.* **2006**, *8*, 18–25.
58. Uça, Z.D.; Erbek, F.S.; Kuşak, L.; Yaşa, F.; Özden, G. The use of optic and radar satellite data for coastal environments. *Int. J. Remote Sens.* **2006**, *27*, 3739–3747.
59. Balik Sanli, F.; Bektas Balcik, F.; Goksel, C. Defining temporal spatial patterns of mega city Istanbul to see the impacts of increasing population. *Environ. Monit. Assess.* **2008**, *146*, 267–275.
60. Karaburun, A.; Demirci, A.; Suen, I.S. Impacts of urban growth on forest cover in Istanbul. *Environ. Monit. Assess.* **2010**, *166*, 267–277.
61. Erbek, F.S.; Ulubay, A.; Maktav, D.; Yağiz, E. The use of satellite image maps for urban planning in Turkey. *Int. J. Remote Sens.* **2005**, *26*, 775–784.
62. Coleman, H.M.; Kanat, G.; Turkdogan, F.I.A. Restoration of the Golden Horn Estuary (Halic). *Water Res.* **2009**, *43*, 4989–5003.
63. Gunay, Z.; Dokmeci, V. Culture-led regeneration of Istanbul waterfront: Golden Horn Cultural Valley Project. *Cities* **2012**, *29*, 213–222.
64. Lykke, S.; Belkaya, H. Marmaray project: The project and its management. ITA/AITES accredited material. *Tunn. Undergr. Space Technol.* **2005**, *20*, 600–603.
65. Sakaeda, H. Marmaray project: Tunnels and stations in BC contract. ITA/AITES accredited material. *Tunn. Undergr. Space Technol.* **2005**, *20*, 612–616.
66. Efe, R.; Cürebal, I. Impacts of the “Marmaray” project (Bosphorus Tube crossing, tunnels and stations) on transportation and urban environment in Istanbul. In *Engineering Earth*; Brunn, S.D., Ed.; Springer Science+Business Media B.V.: Dordrecht, The Netherlands, 2011; pp. 715–733.
67. Oktay, F.Y.; Gokasan, E.; Sakinc, M.; Yaltrak, C.; Imren, C.; Demirbag, E. The effect of North Anatolian Fault Zone to the latest connection between Black Sea and Sea of Marmara. *Mar. Geol.* **2002**, *190*, 367–382.
68. Yildirim, M.; Savaskan, E. Istanbul Tersiyer cokellerinin stratigrafisi ve muhendislik ozellikleri. Uluslararası Muhendislik Jeolojisi Turk Milli Komitesi (MJTMK) Bulteni, 25. Yil, S.18, Istanbul, 2002; pp. 48–62.
69. Özaydın, K.; Edil, T.B.; Yildirim, S.; Uzel, T.; Berilgen, M.M.; Hosbas, G.; Ozcoban, M.S.; Kilic, H. *Behaviour of Embankments on Soft Soils*; Final Research Report to the State Planning Organization: Ankara, Turkey, 1999.
70. Dalgiç, S.; Turgut, M.; Kuşku, İ.; Coşkun, Ç.; Coşgun, T. The effect of soil and rock conditions on construction foundation on the European side of Istanbul. *Uygulamalı Yerbilimleri Sayı* **2009**, *2*, 47–70.
71. Pepe, A.; Lanari, R. On the extension of the minimum cost flow algorithm for phase unwrapping of multitemporal differential SAR interferograms. *IEEE Trans. Geosci. Remote Sens.* **2006**, *44*, 2374–2383.
72. Strang, G. *Linear Algebra and Its Applications*. Harcourt Brace Jovanovich: Orlando, FL, USA, 1988.
73. Imperatore, P.; Pepe, A.; Lanari, R. Multi-Channel phase unwrapping: problem topology and dual-level parallel computational model. *IEEE Trans. Geosci. Remote Sens.* **2015**, *53*, 5774–5793.
74. Walter, T.R.; Manzo, M.; Manconi, A.; Solaro, G.; Lanari, R.; Motagh, M.; Woith, H.; Parolai, S.; Shirazei, M.; Zschau, J.; Baris, S.; Ansal, A. Satellite monitoring of hazards: A focus on Istanbul, Turkey. *Eos, Trans. Am. Geophys. Union* **2010**, *91*, 313–324.
75. Kurt, S.; Karaburun, A.; Demirci, A. Coastline changes in Istanbul between 1987 and 2007. *Sci. Res. Essays* **2010**, *5*, 3009–3017.
76. Istanbul Municipality. Istanbul Turkey. Report on 1/100000 scaled environmental arrangement plan report on Istanbul part 3, Istanbul Metropolitan Municipality, Department of Housing and Urban Development,

2009. Available online: http://www.planlama.org/images/stories/Dokuman/istanbul_cdp/3-b_il_butunu_aras_bulgulari.pdf (accessed on 3 September 2015).
77. Toğrol, E.; Eyigün, Y.; Küman, S. The Creeping Shores of the Golden Horn. In Proceedings of 2nd International Conference on New Developments in Soil Mechanics and Geotechnical Engineering, Nicosia, Cyprus, 28–30 May 2009.
78. Milliyet Gazetesi. Available online: <http://www.milliyet.com.tr/halic-in-vidasicikti/gundem/gundemdetay/23.05.2012/1543765/default.htm> (accessed on 27 October 2015).
79. Hürriyet Gazetesi. Available online: <http://www.hurriyet.com.tr/eyupte-yine-toprak-kaymasi-27885270> (accessed on 27 October 2015).
80. Kılıç, H.; Berilgen, S.; Biçer, P.; Yıldırım, M. Laboratory and Field Observations for Golden Horn Marine Clay. *Mar. Georesour. Geotechnol.* **2010**, *28*, 303–323
81. Özaydın, K.; Yıldırım, M.; Yıldırım S.; Kılıç, H.; Akgüner, C. İstanbul Büyükşehir Belediye Başkanlığı Haliç Islah Projesi—Fizibilite Raporu İçin Taban Çamurunun Geoteknik ve Kirlilik Özelliklerinin Belirlenmesi ve Çamurun Taranması ve Uzaklaştırılması Projesi, 5. Cilt, İstanbul Büyükşehir Belediyesi Arşivi, 1995.
82. Ulaştırma, T.C. Denizcilik ve Haberleşme Bakanlığı Her Hakkı Saklıdır. Settlement contour map. Reference No: BC1-30-11-02-00-5082#00, TGN-AVR-BC1-16630, 02/01/2014.
83. Attema, E.; Bargellini, P.; Edwards, P.; Levrini, G.; Lokas, S.; Moeller, L.; Rosich-Tell, B.; Secchi, P.; Torres, R.; Davidson, M.; Snoeij, P. Sentinel-1: The radar mission for GMES operational land and sea services. *ESA Bull.* **2007**, *131*, 10–17.
84. De Luca, C.; Cuccu, R.; Elefante, S.; Zinno, I.; Manunta, M.; Rivolta, G.; Casola, V.; Lanari, R.; Casu, F. Unsupervised on-demand web service for DInSAR processing: The P-SBAS implementation within the esa G-POD environment. In Proceedings of the International Geoscience And Remote Sensing Symposium (IGARSS), Milan, Italy, 26–31 July 2015.



© 2015 by the authors; licensee MDPI, Basel, Switzerland. This article is an open access article distributed under the terms and conditions of the Creative Commons by Attribution (CC-BY) license (<http://creativecommons.org/licenses/by/4.0/>).